

Research Article

Optimal Sizing and Deployment of Renewable Energy Generators in Practical Transmission Network Using Grid-Oriented Multiobjective Harmony Search Algorithm for Loss Reduction and Voltage Profile Improvements

**Pramod Kumar,¹ Nagendra Kumar Swarnkar,¹ Om Prakash Mahela ^{2,3},
 Baseem Khan ^{3,4}, Divya Anand,^{5,6} Aman Singh,^{6,7} Juan Luis Vidal Mazon ^{6,8}
 and Fahd S. Alharithi ⁹**

¹Department of Electrical Engineering, Suresh Gyan Vihar University, Jaipur, India

²Power System Planning Division, Rajasthan Rajya Vidyut Prasaran Nigam Ltd., Jaipur 302005, Rajasthan, India

³Engineering Research and Innovation Group (ERIG), Universidad Internacional Iberoamericana, Campeche, C.P. 24560, Mexico

⁴Department of Electrical Engineering, Hawassa University, Hawassa, Ethiopia

⁵School of Computer Science and Engineering, Lovely Professional University, Phagwara, Punjab 144411, India

⁶Higher Polytechnic School, Universidad Europea del Atlántico, C/Isabel Torres 21, Santander 39011, Spain

⁷Uttaranchal Institute of Technology, Uttaranchal University, Dehradun 248007, Uttarakhand, India

⁸Department of Engineering, Universidad Internacional Iberoamericana, Arecibo 00613, Puerto Rico, USA

⁹Department of Computer Science, College of Computers and Information Technology, Taif University, P.O. Box 11099, Taif 21944, Saudi Arabia

Correspondence should be addressed to Baseem Khan; baseem.khan1987@gmail.com

Received 23 July 2022; Revised 26 October 2022; Accepted 10 January 2023; Published 22 March 2023

Academic Editor: Lalit Chandra Saikia

Copyright © 2023 Pramod Kumar et al. This is an open access article distributed under the Creative Commons Attribution License, which permits unrestricted use, distribution, and reproduction in any medium, provided the original work is properly cited.

This paper presents grid-oriented multiobjective harmony search algorithm (GOMOHSA) to incorporate the multiple grid parameters for minimization of the active power loss, reactive power loss, and total voltage deviations (TVD) in a part of practical transmission network of Rajasthan Rajya Vidyut Prasaran Nigam Limited (RVPN) in southern parts of Rajasthan state of India. This is achieved by optimal deployment of optimally sized renewable energy (RE) generators using GOMOHSA. Performance indexes such as active power loss minimization index (APMLI), the reactive power loss minimization index (RPLMI), and the total voltage deviation improvement index (TVDII) are introduced to evaluate the health of the test network with different load scenarios. Performance of proposed GOMOHSA has been tested for five different operating scenarios of loads and RE generation. It is established that the proposed GOMOHSA finds the optimal deployment of optimally sized RE generators, and the investment cost of deployment of these RE generators can be recovered within a time period that is less than 5 years. Performance of GOMOHSA is superior compared to a conventional genetic algorithm (GA) in terms of performance indexes, RE generator capacity, payback period, and parameter sensitivity. Study is performed using MATLAB software for loading scenario of base year 2021 and projected year 2031.

1. Introduction

Rapid growth in the use of electrical energy globally has affected the operation of electric power networks. To mitigate the gap between demand and supply, use of the renewable energy (RE) sources has been pronounced. Furthermore, environmental issues have also forced the power utilities to integrate high-capacity wind and solar parks to the network of utilities. Optimal placement of renewable energy generator (REG) having optimal capacity will provide reliable and effective operation of power system networks. Integration of a REG to the grid near the load will minimize the losses and improve power factor. Practically, wind and solar power plants can be installed at the locations where wind and solar resources are available in abundance [1]. Therefore, optimal deployment of REGs having optimal sizes in the existing power system network is a complex task and detailed analysis of the network and system parameters is required for different scenarios. Multiple studies are reported which supports the sizing and placing of REGs in the network of power utilities. In [2], authors developed an optimal locator index (OLI) for optimal location and sizes of distributed energy generators considering the power loss sensitivities and Kalman filter algorithm. An optimal locator index (OLI) is designed for determination of optimal locations of REGs in a systematic and effective manner. Study is validated on a part of practical distribution network of 60 MVA scale located at Do-Gok region in Seoul, Korea. A study proposing the framework to determine optimal sizes and deployment of Battery Energy Storage System (BESS) in the network of power systems considering the uncertainty of generation, demand, intermittent RE generation sources, and contingency locations is introduced in [3]. This study effectively determined the optimal BESS size and location using the quantum and location of critical system loads. It is established that optimal BESS size should be limited to 4.5% of total system loads, and optimal BESS placement is achieved when BESS is deployed near to around 30% of the system loads. In [4], authors designed a technique for identification of optimal location and sizes of REGs using a power stability index (PSI) and particle swarm optimization (PSO) algorithm. This is achieved by designing a maximum power stability index (MPSI), which is derived by application of maximum power transfer theorem. The MPSI index is comparable with other voltage stability indexes and performs better compared to the loss minimization method. A detailed study of techniques employed for placement and sizing of REG units in the power network of utilities is presented in [5]. Algorithms of techniques including analytical optimization technique, heuristic optimization techniques (harmony search, tabu search, simulated annealing, and ant colony optimization), and evolutionary computation techniques (genetic algorithm, differential evolution, and particle swarm optimization) are detailed in this study. Further, a comparative study of the heuristic optimization technique and evolutionary computation techniques is also presented. In [6], a GA technique for optimal location and sizing of DG in the

utility network of a distribution company is presented for different load conditions. This has achieved the acceptable reliability level and voltage profile in the network. In [7], authors designed a hybrid optimization using the particle swarm optimization (PSO) and the salp swarm algorithm (SSA) for maximizing the savings through reconfiguration and optimal placement of RE generators. Economy maximization by minimization of the loss is achieved by application of designed algorithm in the IEEE-119 and IEEE-136 test networks. The application of the artificial bee colony (ABC) technique to decide the optimal location and sizes of RE generators to minimize loss in the power distribution network and improve the voltage profile in a 57 bus network is introduced in [6]. In [8], authors designed a method for minimization of real power loss and net reactive power flow by optimal allocation of DGs and shunt capacitors. This method has achieved the improvement in system performance, reliability, increased loading capacity, and reduction of losses. In [9], authors designed an optimized framework by application of differential evolution algorithm for optimal deployment of multiple DG resources in the distribution grid. This helps to minimize network losses and maximize DG capacity integration to the grid. In [10], authors used the particle artificial bee colony algorithm (PABC) to design a hybrid harmony search algorithm for overcoming the drawbacks of premature and slow convergence of harmony search algorithm (HSA) over multimodel fitness landscape for optimal placement and sizes of the DG units as well as shunt capacitors. Minimum power loss in radial distribution networks and voltage profile are effectively achieved using the proposed method. Results are effectively validated on the IEEE-33 and 119 node test feeders. In [11], authors applied a modification in the traditional firefly approach by proposing formulas for tuning the algorithm parameters and updating equations for optimal size determination and placing the voltage-controlled DG units in both the balanced and unbalanced distribution networks. This method is effective to deal with the practically constrained optimization problems. Power loss minimization in the IEEE-69, 37, and 123 nodes test systems is effectively achieved by DG placement. In [12], authors introduced a multiobjective velocity-based butterfly optimization algorithm for optimal integration of dispatchable distributed generations (DDG) to the power system network to minimize the active power loss, voltage improvement and minimize the annual economic loss. A hybrid fuzzy-metaheuristic method to estimate the optimal size and Location of DG units in the power network to achieve the active and reactive power loss is introduced in [13]. This is achieved by merging fuzzy logic (FL) to adapt weights of objective function dynamically the meta-heuristic equilibrium optimizer. This has merit of high speed of convergence, least execution time, and most consistent results. DG placement techniques such as sustainability-oriented multiobjective optimization model [14] and the genetic algorithm [15, 16] are reported in the literature in recent years.

In a detailed analysis of the literature review discussed in the above paragraph, it is pointed out that optimization

techniques can be modified to include grid parameters for optimal sizing and deployment of RE generators in the practical transmission networks. This has been considered as the research objective in this paper, and the following are the main contributions of this paper:

- (i) Harmony search algorithm (HSA) is modified to incorporate the multiobjective functions to minimize the active power loss, reactive power loss, and total voltage deviations (TVD) in the practical transmission network. Modified HSA includes the multiple grid parameters; hence, it is designated as grid-oriented multiobjective harmony search algorithm (GOMOHSA).
- (ii) Proposed algorithm is effectively implemented for optimal deployment of optimally sized RE generators in the RVPN practical transmission network in the southern part of Rajasthan, India. This has been achieved by the application of GOMOHSA with minimum active power loss, minimum reactive power loss, and minimum total voltage deviations.
- (iii) Performance indexes such as the active power loss minimization index (APMLI), the reactive power loss minimization index (RPMLI), and the total voltage deviation improvement index (TVDII) are introduced to evaluate the health of the test network with different load scenarios.
- (iv) Performance of the proposed GOMOHSA has been tested for five different operating scenarios of loads and RE generation for the base year 2021 and the projected year 2031.
- (v) It is established that the proposed GOMOHSA finds the optimal deployment of optimally sized RE generators, and the investment cost of the deployment of these RE generators can be recovered within a time period less than 5 years.
- (vi) Performance of GOMOHSA is superior compared to the conventional genetic algorithm (GA) in terms of performance indexes, RE generator capacity, and payback period.

This article is arranged into eight sections. Introduction, review of literature, and research contribution are included in Section 1. Practical test utility network configuration and relevant data of transformers, transmission lines, generation, loads, and RE generator are described in Section 2. Computation of load projections for the projected year 2031 is detailed in Section 3. The proposed grid-oriented multiobjective harmony search algorithm with relevant mathematical formulations is described in Section 4. This section also discussed the grid performance parameters used to evaluate health of the test network during different scenario of loads. Detailed simulation results and discussion is included in Section 5. The analysis of cost benefits used to estimate the payback period for the investments incurred on the deployment of RE generators is presented in Section 6. A performance comparative study is included in Section 7. Research findings are concluded in Section 8 of the article.

2. Test Utility Grid Network

A transmission system owned by Rajasthan Rajya Vidyut Prasaran Nigam Limited (RVPN) in the Udaipur region, along with private generators in the region is used to perform the proposed study. The RVPN transmission system is operated at 132 kV, 220 kV, 400 kV, and 765 kV voltage levels [17]. Technical parameters, including circuit length of transmission lines, voltage levels, generation capacity, and transformer details reported in [17, 18], are used for the proposed study. The transmission network used for this study has 70 nodes, and the interconnection of lines with different buses along with generators and loads is described in Figure 1. The 2 nodes are operated at 400 kV voltages, 11 nodes are maintained at 220 kV voltages, and 57 nodes are maintained at 132 kV voltages. Loads are connected to the buses operated at 132 kV voltages and realized by PQ type nature. Details of buses (name and number), bus voltage level, load detail, and shunt reactive compensation are included in Tables 1 and 2 [17]. Symbols L1 to L57 are used to represent the loads connected to the utility network. Recorded peak loads on the 132 kV buses for the financial year (FY) 2021-2022 are also included in Tables 1 and 2 [17]. Since, peak load is not simultaneously recorded on all the buses, hence, 70% of the peak loads is taken to represent the average load of the system. Hence, the system load for the study corresponding to FY 2021-2022 is taken to be equal to 498.33 MW. Bus-1 and bus-2 are connected to rest of the network. Hence, the net exchange of power between network considered for the study and the rest of the network is represented by generators GEN-1 and GEN-2 at bus-1 and bus-2, respectively.

Generators integrated to the test utility grid including the bus number, bus name, symbol of generator, voltage level of generator bus, active power rating of generator, and reactive power rating of the generator are described in Table 3. Symbols UGEN-1 to UGEN-8 is assigned to the generators.

Transmission line details, including the from and to bus numbers, symbol of transmission line, voltage level, line length, type of conductor, and type of circuit (single circuit (S/C) or double circuit (D/C)) are described in Tables 4 and 5. These transmission lines are operated at voltage levels of 132 kV, 220 kV, and 400 kV.

Aluminium conductor steel-reinforced (ACSR) equivalent panther conductor is used for the 132 kV lines, and ACSR equivalent zebra conductor is used for the 220 kV lines. A twin moose conductor is used for the 400 kV transmission line connected between bus-1 and bus-2. Details of the conductors used for the transmission lines, including the resistance, reactance, and thermal rating used for the study are reported in [19, 20]. These data are included in Table 6. The thermal rating of the line is the power rating for which transmission lines can be operated continuously.

Technical parameters of the transformers connected in the test network, buses between which transformers are installed, transformer MVA rating, impedance including positive sequence (Z_1), zero sequence (Z_0), ratio of positive sequence reactance (X_1) to positive sequence resistance (R_1), and ratio of zero sequence reactance (X_0) to zero sequence resistance (R_0) are included in Table 7.

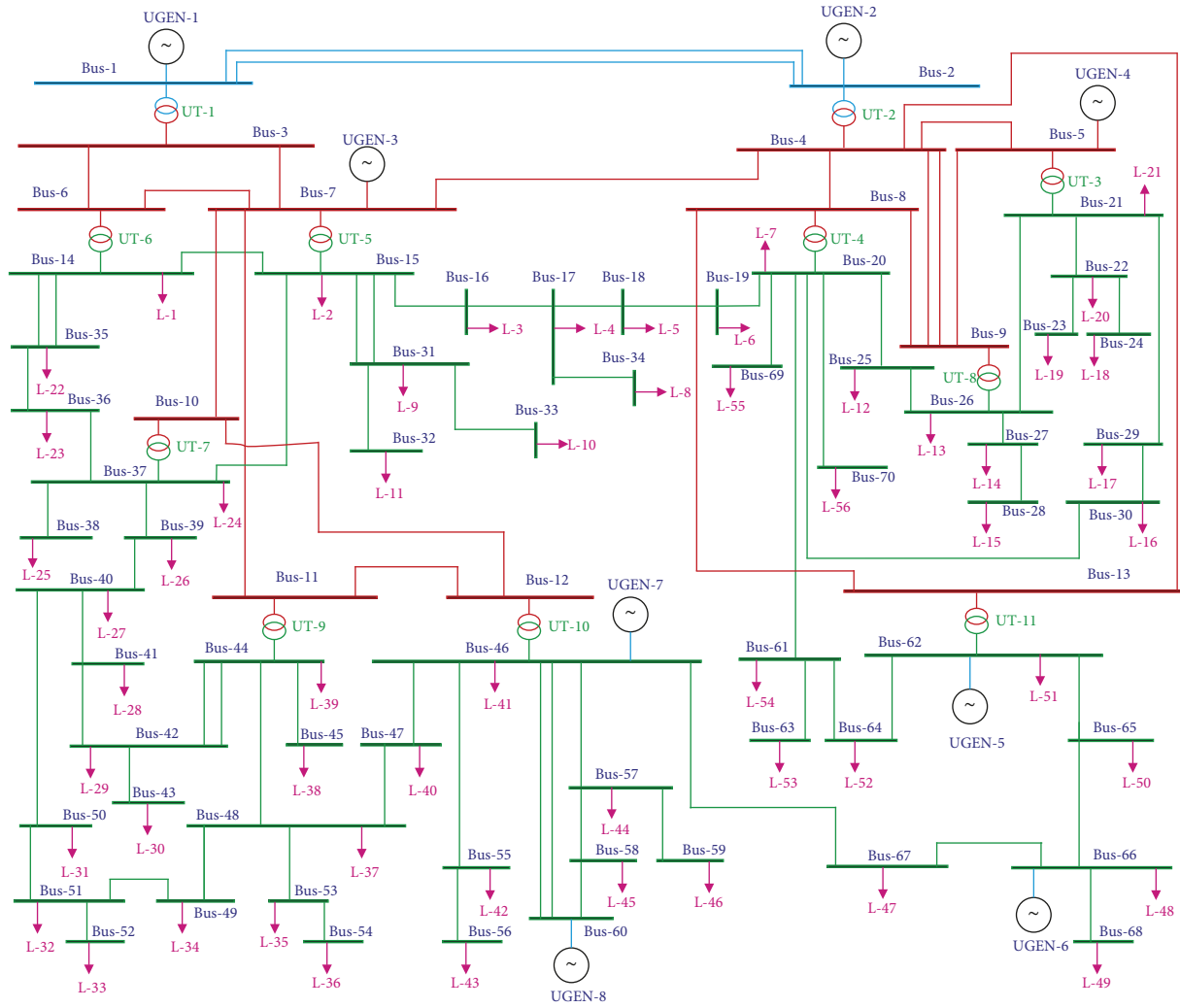


FIGURE 1: Transmission utility network in southern part of Rajasthan (Udaipur), India [17].

TABLE 1: Details of test system buses and loads (part-A) [17].

| Node no. | Node name | Voltage (kV) | Symbol of load | Base year load | | Projected load | |
|----------|---------------------------------|--------------|----------------|----------------|----------|----------------|--------------|
| | | | | P (MW) | Q (MVAR) | Pload (MW) | Qload (MVAR) |
| 1 | 400 kV Kankroli (PGCIL) | 400 | — | — | — | — | — |
| 2 | 400 kV Chittorgarh (RVPN) | 400 | — | — | — | — | — |
| 3 | 220 kV Kankroli (400 kV GSS) | 220 | — | — | — | — | — |
| 4 | 220 kV Chittorgarh (400 kV GSS) | 220 | — | — | — | — | — |
| 5 | 220 kV Chittorgarh (220 kV GSS) | 220 | — | — | — | — | — |
| 6 | 220 kV Amberi | 220 | — | — | — | — | — |
| 7 | 220 kV Debari | 220 | — | — | — | — | — |
| 8 | 220 kV Nimbahera | 220 | — | — | — | — | — |
| 9 | 220 kV Sawa | 220 | — | — | — | — | — |
| 10 | 220 kV Madri | 220 | — | — | — | — | — |
| 11 | 220 kV Aspur | 220 | — | — | — | — | — |
| 12 | 220 kV Banswara | 220 | — | — | — | — | — |
| 13 | 220 kV Pratapgarh | 220 | — | — | — | — | — |
| 14 | 132 kV Amberi | 132 | L-1 | 10.593 | 5.130 | 14.647 | 7.093 |
| 15 | 132 kV Debari | 132 | L-2 | 71.326 | 16.991 | 98.622 | 23.493 |
| 16 | 132 kV Bhatewar | 132 | L-3 | 30.225 | 9.972 | 41.792 | 13.788 |
| 17 | 132 kV Bhinder | 132 | L-4 | 24.879 | 14.202 | 34.400 | 19.637 |
| 18 | 132 kV Mangalwad | 132 | L-5 | 26.560 | 14.738 | 36.724 | 20.378 |

TABLE 1: Continued.

| Node no. | Node name | Voltage (kV) | Symbol of load | Base year load | | Projected load | |
|----------|-------------------------|--------------|----------------|----------------|-----------------|----------------|--------------|
| | | | | <i>P</i> (MW) | <i>Q</i> (MVAR) | Pload (MW) | Qload (MVAR) |
| 19 | 132 kV Dhoriya Chauraha | 132 | L-6 | 10.593 | 5.130 | 14.647 | 7.093 |
| 20 | 132 kV Nimbahera | 132 | L-7 | 60.585 | 28.468 | 83.771 | 39.363 |
| 21 | 132 kV Chittorgarh | 132 | L-21 | 47.894 | 17.252 | 66.223 | 23.854 |
| 22 | 132 kV Ajoliya Khera | 132 | L-20 | 24.361 | 11.031 | 33.684 | 15.253 |
| 23 | 132 kV Bassi | 132 | L-19 | 13.700 | 6.635 | 18.943 | 9.174 |
| 24 | 132 kV Rashmi | 132 | L-18 | 14.741 | 8.354 | 20.382 | 11.551 |
| 25 | 132 kV Bhadesar | 132 | L-12 | 16.659 | 9.135 | 23.034 | 12.631 |
| 26 | 132 kV Sawa | 132 | L-13 | 22.634 | 6.669 | 31.296 | 9.221 |
| 27 | 132 kV Kapasan | 132 | L-14 | 28.469 | 21.892 | 39.364 | 30.270 |
| 28 | 132 kV Bhopalsagar | 132 | L-15 | 10.593 | 5.130 | 14.647 | 7.093 |
| 29 | 132 kV Senth | 132 | L-17 | 14.166 | 5.752 | 19.587 | 7.953 |
| 30 | 132 kV Rasoolpura | 132 | L-16 | 52.937 | 11.815 | 73.196 | 16.337 |
| 31 | 132 kV Mavli | 132 | L-9 | 22.019 | 9.908 | 30.446 | 13.699 |
| 32 | 132 kV Sanwad | 132 | L-11 | 14.745 | 6.787 | 20.388 | 9.384 |
| 33 | 132 kV Dariba | 132 | L-10 | 17.740 | 11.310 | 24.529 | 15.638 |
| 34 | 132 kV Joojhpura | 132 | L-8 | 10.593 | 5.130 | 14.647 | 7.093 |
| 35 | 132 kV Sukher | 132 | L-22 | 36.136 | 17.502 | 49.965 | 24.200 |
| 36 | 132 kV Pratapnagar | 132 | L-23 | 36.970 | 10.539 | 51.118 | 14.572 |
| 37 | 132 kV Madri | 132 | L-24 | 40.515 | 16.511 | 56.020 | 22.829 |
| 38 | 132 kV Dakan Kotda | 132 | L-25 | 15.148 | 4.760 | 20.945 | 6.581 |
| 39 | 132 kV Balicha | 132 | L-26 | 10.593 | 5.130 | 14.647 | 7.093 |
| 40 | 132 kV Zawarmines | 132 | L-27 | 10.868 | 5.264 | 15.027 | 7.278 |
| 41 | 132 kV Sarada | 132 | L-28 | 5.261 | 0.468 | 7.274 | 0.647 |
| 42 | 132 kV Salumber | 132 | L-29 | 19.290 | 9.343 | 26.672 | 12.918 |
| 43 | 132 kV Bambora | 132 | L-30 | 10.593 | 5.130 | 14.647 | 7.093 |
| 44 | 132 kV Aspur | 132 | L-39 | 9.677 | 2.354 | 13.380 | 3.255 |
| 45 | 132 kV Dhariyawad | 132 | L-38 | 11.426 | 6.695 | 15.798 | 9.257 |
| 46 | 132 kV Banswara | 132 | L-41 | 52.944 | 18.863 | 73.206 | 26.082 |
| 47 | 132 kV Partapur | 132 | L-40 | 12.676 | 6.808 | 17.527 | 9.413 |
| 48 | 132 kV Sagwara | 132 | L-37 | 18.926 | 8.397 | 26.169 | 11.611 |
| 49 | 132 kV Dungarpur | 132 | L-34 | 29.710 | 9.004 | 41.080 | 12.449 |
| 50 | 132 kV Rishbhdeo | 132 | L-31 | 24.858 | 8.199 | 34.371 | 11.36 |

TABLE 2: Details of test system buses and loads (part-B) [17].

| Node no. | Node name | Voltage (kV) | Symbol of load | Base year load | | Projected load | |
|----------|--------------------|--------------|----------------|----------------|-----------------|----------------|--------------|
| | | | | <i>P</i> (MW) | <i>Q</i> (MVAR) | Pload (MW) | Qload (MVAR) |
| 51 | 132 kV Kherwara | 132 | L-32 | 10.289 | 0.791 | 14.227 | 1.094 |
| 52 | 132 kV Bichiwara | 132 | L-33 | 6.292 | 0.833 | 8.699 | 1.152 |
| 53 | 132 kV Chitri | 132 | L-35 | 10.593 | 5.130 | 14.647 | 7.093 |
| 54 | 132 kV Seemalwara | 132 | L-36 | 12.161 | 1.688 | 16.815 | 2.334 |
| 55 | 132 kV Paloda | 132 | L-42 | 7.627 | 3.694 | 10.546 | 5.108 |
| 56 | 132 kV Ghatol | 132 | L-43 | 5.198 | 1.497 | 7.188 | 2.069 |
| 57 | 132 kV Bagidora | 132 | L-44 | 10.480 | 5.919 | 14.491 | 8.184 |
| 58 | 132 kV Chordi | 132 | L-45 | 10.00 | 4.00 | 13.827 | 5.531 |
| 59 | 132 kV Kushalgarh | 132 | L-46 | 9.181 | 1.836 | 12.694 | 2.5386 |
| 60 | 132 kV Mahi-II | 132 | — | — | — | — | — |
| 61 | 132 kV Chhotisadri | 132 | L-54 | 21.391 | 10.720 | 29.577 | 14.822 |
| 62 | 132 kV Pratapgarh | 132 | L-51 | 34.943 | 17.584 | 48.315 | 24.313 |
| 63 | 132 kV Badisadri | 132 | L-53 | 23.008 | 5.089 | 31.813 | 7.036 |
| 64 | 132 kV Barawada | 132 | L-52 | 10.001 | 4.002 | 13.828 | 5.533 |
| 65 | 132 kV Mokhampura | 132 | L-50 | 10.593 | 5.130 | 14.647 | 7.093 |
| 66 | 132 kV Dalot | 132 | L-48 | 18.810 | 11.657 | 26.008 | 16.118 |
| 67 | 132 kV Peeplawa | 132 | L-47 | 10.593 | 5.130 | 14.647 | 7.093 |
| 68 | 132 kV Negadiya | 132 | L-49 | 10.593 | 5.130 | 14.647 | 7.093 |
| 69 | 132 kV Bijapur | 132 | L-55 | 10.595 | 5.110 | 14.649 | 7.065 |
| 70 | 132 kV Kanera | 132 | L-56 | 9.004 | 4.361 | 12.449 | 6.029 |

TABLE 3: Details of generators connected to test system.

| Bus no. | Bus names | Generator symbol | Voltage (kV) | P (MW) generated | Q (MVAR) generated |
|---------|---------------------------|------------------|--------------|--------------------|----------------------|
| 1 | 400 kV Kankroli (PGCIL) | UGEN-1 | 400 | 120 | 25 |
| 2 | 400 kV Chittorgarh (RVPN) | UGEN-2 | 400 | 430 | 20 |
| 7 | 220 kV Debari | UGEN-3 | 220 | 210 | 10 |
| 5 | 220 kV Chittorgarh (RVPN) | UGEN-4 | 220 | 200 | 10 |
| 62 | 132 kV Pratapgarh | UGEN-5 | 132 | 60 | 0.02 |
| 66 | 132 kV Dalot | UGEN-6 | 132 | 31.25 | 0.02 |
| 46 | 132 kV Banswara | UGEN-7 | 132 | 32 | 10 |
| 60 | 132 kV Mahi-II | UGEN-8 | 132 | 60 | 15 |

TABLE 4: Description of transmission lines (part-A).

| Transmission line symbol | From node no. | To node no. | Voltage level (kV) | Line length (km) | Conductor type | Line circuit type |
|--------------------------|---------------|-------------|--------------------|------------------|----------------|-------------------|
| TL-1 | 1 | 2 | 400 | 71.03 | Twin moose | D/C |
| TL-2 | 3 | 6 | 220 | 63.00 | ACSR zebra | S/C |
| TL-3 | 6 | 7 | 220 | 30.00 | ACSR zebra | S/C |
| TL-4 | 7 | 4 | 220 | 90.00 | ACSR zebra | S/C |
| TL-5 | 4 | 8 | 220 | 50.00 | ACSR zebra | S/C |
| TL-6 | 4 | 5 | 220 | 10.10 | ACSR zebra | S/C |
| TL-7 | 4 | 13 | 220 | 120.00 | ACSR zebra | S/C |
| TL-8 | 4 | 9 | 220 | 25.00 | ACSR zebra | D/C |
| TL-9 | 5 | 9 | 220 | 25.00 | ACSR zebra | S/C |
| TL-10 | 8 | 9 | 220 | 21.50 | ACSR zebra | S/C |
| TL-11 | 8 | 13 | 220 | 80.94 | ACSR zebra | S/C |
| TL-12 | 7 | 10 | 220 | 25.60 | ACSR zebra | S/C |
| TL-13 | 7 | 11 | 220 | 91.96 | ACSR zebra | S/C |
| TL-14 | 10 | 12 | 132 | 156.90 | ACSR zebra | S/C |
| TL-15 | 14 | 15 | 132 | 17.50 | ACSR panther | S/C |
| TL-16 | 15 | 16 | 132 | 26.50 | ACSR panther | S/C |
| TL-17 | 16 | 17 | 132 | 31.80 | ACSR panther | S/C |
| TL-18 | 17 | 18 | 132 | 22.00 | ACSR panther | S/C |
| TL-19 | 18 | 19 | 132 | 25.00 | ACSR panther | S/C |
| TL-20 | 19 | 20 | 132 | 25.00 | ACSR panther | S/C |
| TL-21 | 20 | 25 | 132 | 27.22 | ACSR panther | S/C |
| TL-22 | 20 | 30 | 132 | 7.35 | ACSR panther | S/C |
| TL-23 | 20 | 61 | 132 | 28.00 | ACSR panther | S/C |
| TL-24 | 20 | 69 | 132 | 47.94 | ACSR panther | S/C |
| TL-25 | 20 | 70 | 132 | 46.64 | ACSR panther | S/C |
| TL-26 | 25 | 26 | 132 | 23.22 | ACSR panther | S/C |
| TL-27 | 26 | 27 | 132 | 32.82 | ACSR panther | S/C |
| TL-28 | 26 | 21 | 132 | 21.00 | ACSR panther | S/C |
| TL-29 | 27 | 28 | 132 | 15.00 | ACSR panther | S/C |
| TL-30 | 21 | 22 | 132 | 13.40 | ACSR panther | S/C |
| TL-31 | 21 | 29 | 132 | 11.00 | ACSR panther | S/C |
| TL-32 | 22 | 23 | 132 | 13.28 | ACSR panther | S/C |
| TL-33 | 22 | 24 | 132 | 28.00 | ACSR panther | S/C |
| TL-34 | 29 | 30 | 132 | 23.35 | ACSR panther | S/C |
| TL-35 | 17 | 34 | 132 | 22.99 | ACSR panther | S/C |
| TL-36 | 15 | 31 | 132 | 33.84 | ACSR panther | D/C |
| TL-37 | 31 | 32 | 132 | 16.74 | ACSR panther | S/C |
| TL-38 | 31 | 33 | 132 | 23.80 | ACSR panther | S/C |
| TL-39 | 14 | 35 | 132 | 6.50 | ACSR panther | D/C |
| TL-40 | 35 | 36 | 132 | 8.34 | ACSR panther | S/C |
| TL-41 | 36 | 37 | 132 | 5.71 | ACSR panther | S/C |
| TL-42 | 37 | 38 | 132 | 9.37 | ACSR panther | S/C |
| TL-43 | 37 | 39 | 132 | 22.00 | ACSR panther | S/C |
| TL-44 | 39 | 40 | 132 | 22.00 | ACSR panther | S/C |
| TL-45 | 40 | 50 | 132 | 34.00 | ACSR panther | S/C |
| TL-46 | 40 | 41 | 132 | 16.00 | ACSR panther | S/C |
| TL-47 | 41 | 42 | 132 | 17.33 | ACSR panther | S/C |
| TL-48 | 42 | 43 | 132 | 25.00 | ACSR panther | S/C |
| TL-49 | 42 | 44 | 132 | 38.52 | ACSR panther | D/C |
| TL-50 | 44 | 45 | 132 | 64.52 | ACSR panther | S/C |
| TL-51 | 44 | 48 | 132 | 46.60 | ACSR panther | S/C |
| TL-52 | 48 | 53 | 132 | 23.00 | ACSR panther | S/C |
| TL-53 | 53 | 54 | 132 | 23.00 | ACSR panther | S/C |

2.1. RE Generator. A solar photovoltaic power plant (SPP) is used for this study. The basic block scheme of the proposed SPP is detailed in Figure 2. Solar energy is trapped by the solar photovoltaic (PV) plates and converted into electrical power of a DC nature at a lower voltage. This DC power is converted to a higher DC voltage using the DC to DC converter, which is further converted to AC power using an inverter. Filters are used to filter out the undesired harmonic components. AC power is supplied to the utility grid, and a transformer may be used to match the AC voltage levels of the inverter and utility grid.

Details and technical parameters of the solar PV plates, array configuration, DC-DC converter, inverter, filter, and transformers used for the study are available in [21–23].

3. Load Projection

The average load recorded on the buses of the test network during five consecutive years is included in Table 8. Furthermore, the average annual load growth rate (ALGR) is also included in Table 8. Load projection curve is illustrated in Figure 3. Careful analysis of the data included in Table 8 indicates that average load as well as ALGR both increases continuously year-on-year basis. The linear fitting method of the curve fitting tool of MATLAB software is used to forecast the loads for a period of ten years (from year 2022 to year 2031). This method used the best-fit linear model using least square approximation technique for computing the load projections. A mathematical description of this technique is presented in [24, 25].

The following equation is used by the linear fit mathematical model for computation of projected average load (PAL) for time horizon of ten years from year 2022 to the year 2031.

$$\text{PAL}(x) = a \times (\sin(x - \pi)) + b \times ((x - 10)^2) + c, \quad (1)$$

where x indicates the load projection year; $a = 8.276$; $b = 0.01107$; $c = -4.364 \times 10^4$. Here, coefficients a , b , and c are estimated with 95% confidence limits. The summation of squared estimate of errors (SSE) is equal to 2.776. The root mean square error (RMSE) is 1.178. R -square is equal to 0.9999. The magnitude of R -square near to unity is a strong indication that load projections are obtained with high accuracy level. A computed total projected load for the test network over a ten years' time horizon is provided in Table 9. Furthermore, load projections reflected on individual buses of the test network are included in Tables 1 and 2.

4. Proposed GOMOHSA Method and Performance Indexes

The proposed method of grid-oriented multiobjective harmony search algorithm (GOMOHSA) used for deployment of RE generators in a practical transmission network of RVPN to improve voltage profile and minimize losses is described in this section. Further, performance function indexes used to evaluate improvements in the grid's health are also described in this Section.

4.1. Objective Function Formulation. The main objectives of the proposed study are the minimization of network active power loss, minimization of network reactive power loss, and the improvement in voltage profile by the minimization of total voltage deviations. These three objective functions are described in this section.

Active power loss minimization function (APF) is expressed by the following expression:

$$\text{APF} = \sum_{i=1}^m (I_{i,\text{real}}^2 \times R_i). \quad (2)$$

Reactive power loss minimization function (RPF) is expressed by the following expression:

$$\text{RPF} = \sum_{i=1}^m (I_{i,\text{img}}^2 \times R_i). \quad (3)$$

Total voltage deviation minimization function (TVDF) is expressed by the following expression:

$$\text{TVDF} = \sum_{i=1}^m (1 - V_i)^2. \quad (4)$$

4.1.1. Constraints. Optimal deployment of RE generators having optimal sizes has been achieved with constraint limits of bus voltages, RE generator capacity, thermal limits of transmission lines, active power loss constraints, and reactive power loss constraints. Bus voltage limits are defined as follows:

$$V_i^{\min} \leq V_i \leq V_i^{\max}. \quad (5)$$

Voltage limits are considered between 97% and 103% of rated voltage of each bus as per Indian electricity grid codes. Thermal limit constraint of transmission line is defined by the following relation:

$$I_{i,j} \leq I_{\text{rated}}. \quad (6)$$

Thermal limits used for the transmission lines are considered as specified in transmission planning criteria for the Indian transmission network [20]. Limit for RE generators is defined by the following relation:

$$S_{DG_i}^{\min} \leq S_{DG_i} \leq S_{DG_i}^{\max}, \quad (7)$$

where maximum and minimum limits for RE generator capacity are considered as 50MW and 200MW, respectively.

Active power loss constraint is defined in terms of active power loss in the presence of RE generator (P_{L-DG}) and active power loss in the absence of RE generator placement ($P_{L-\text{without-DG}}$) by following relation:

$$P_{L-DG} \leq P_{L-\text{without-DG}}. \quad (8)$$

Reactive power loss constraint is defined in terms of reactive power loss in the presence of RE generator (Q_{L-DG}) and reactive power loss in the absence of RE generator placement ($Q_{L-\text{without-DG}}$) by following relation:

TABLE 5: Description of transmission lines (part-B).

| Transmission line symbol | From node no. | To node no. | Voltage level (kV) | Line length (km) | Conductor type | Line circuit type |
|--------------------------|---------------|-------------|--------------------|------------------|----------------|-------------------|
| TL-54 | 48 | 49 | 132 | 46.60 | ACSR panther | S/C |
| TL-55 | 49 | 51 | 132 | 25.62 | ACSR panther | S/C |
| TL-56 | 51 | 52 | 132 | 21.3 | ACSR panther | S/C |
| TL-57 | 51 | 50 | 132 | 30.02 | ACSR panther | S/C |
| TL-58 | 46 | 47 | 132 | 36.11 | ACSR panther | S/C |
| TL-59 | 47 | 48 | 132 | 37.46 | ACSR panther | S/C |
| TL-60 | 46 | 55 | 132 | 35.47 | ACSR panther | S/C |
| TL-61 | 55 | 56 | 132 | 40.50 | ACSR panther | S/C |
| TL-62 | 46 | 60 | 132 | 42.00 | ACSR panther | D/C |
| TL-63 | 46 | 57 | 132 | 22.40 | ACSR panther | S/C |
| TL-64 | 57 | 59 | 132 | 31.63 | ACSR panther | S/C |
| TL-65 | 57 | 58 | 132 | 4.90 | ACSR panther | S/C |
| TL-66 | 58 | 60 | 132 | 5.00 | ACSR panther | S/C |
| TL-67 | 46 | 67 | 132 | 8.47 | ACSR panther | S/C |
| TL-68 | 67 | 66 | 132 | 21.50 | ACSR panther | S/C |
| TL-69 | 66 | 68 | 132 | 35.00 | ACSR panther | S/C |
| TL-70 | 66 | 65 | 132 | 54.00 | ACSR panther | S/C |
| TL-71 | 65 | 62 | 132 | 20.85 | ACSR panther | S/C |
| TL-72 | 62 | 64 | 132 | 10 | ACSR panther | S/C |
| TL-73 | 64 | 61 | 132 | 12.68 | ACSR panther | S/C |
| TL-74 | 61 | 63 | 132 | 22.68 | ACSR panther | S/C |

TABLE 6: Description of conductors of transmission lines.

| S. no. | Details of technical parameters | Numerical magnitudes of technical parameter used for line conductors | | |
|--------|-------------------------------------|--|--|--|
| | | Twin moose | ACSR zebra | ACSR panther |
| 1 | Positive sequence resistance (R1) | 0.0298 Ω/km/circuit | 0.0749 Ω/km/circuit | 0.1622 Ω/km/circuit |
| 2 | Positive sequence reactance (X1) | 0.332 Ω/km/circuit | 0.3992 Ω/km/circuit | 0.3861 Ω/km/circuit |
| 3 | Positive sequence susceptance (B/2) | $1.7344 \times 10^{-6} \bar{\sigma}$ /km/circuit | $1.4670 \times 10^{-6} \bar{\sigma}$ /km/circuit | $1.4635 \times 10^{-6} \bar{\sigma}$ /km/circuit |
| 4 | Zero sequence resistance (R0) | 0.1619 Ω/km/circuit | 0.2200 Ω/km/circuit | 0.4056 Ω/km/circuit |
| 5 | Zero sequence reactance (X0) | 1.24 Ω/km/circuit | 1.3392 Ω/km/circuit | 1.6222 Ω/km/circuit |
| 6 | Zero sequence susceptance | $1.12 \times 10^{-6} \bar{\sigma}$ /km/circuit | $9.2004 \times 10^{-7} \bar{\sigma}$ /km/circuit | $1.3171 \times 10^{-7} \bar{\sigma}$ /km/circuit |
| 7 | Line thermal rating | 515 MVA | 176 MVA | 71 MVA |

$$Q_{L-DG} \leq Q_{L-without-DG} \quad (9)$$

4.2. *Grid-Oriented Multiobjective Harmony Search Algorithm.* The GOMOHSA is implemented for optimal placement and sizing of RE generators to minimize the total voltage deviations, active power loss, and reactive power loss. The algorithm is implemented for the base network of year 2021 and the projected network of year 2031. Following modifications are applied to the conventional harmony search algorithm to design the GOMOHSA:

- (i) Critical grid parameters such voltage deviation, active power loss and reactive power loss are considered to design the research objective function
- (ii) The grid coordinates (V , P , and Q) are utilized by GOMOHSA to locate individuals in the objective space
- (iii) Constraint limits of the objective are recognized in whole population to set the grid structure of objective functions

(iv) To compute fitness, three grid dependent criteria such as grid ranking (GR), grid crowding distance, and grid coordinate point distance are used by the GOMOHSA to rank the individuals with better fitness

(v) Convergence is computed utilizing the GR and grid coordinate point distance (GCPD)

(vi) Grid crowding distance (GCD) is utilized for computing the diversity of entities

The grid coordinates are utilized by GOMOHSA to locate individuals in the objective space. Constraint limits of the objective are recognized in whole population to set the grid structure of objective functions. Lower and upper limits of grid in the objective are determined as follows [26].

$$ll_k = P_m^{\min} - \frac{(P_m^{\max} - P_m^{\min})}{2 \times \text{NDOS}}, \quad (10)$$

where ll_k : lower limit of k^{th} objective; ul_k : upper limit of k^{th} objective; NDOS: number of divisions of objective space; P_m^{\min} : minimum range of k^{th} objective; P_m^{\max} : maximum range of k^{th} objective

TABLE 7: Description of transformers.

| From node no. | To node no. | Transformer symbol | Voltage ratio (kV) | MVAR capacity (MVA) | Values of transformer parameters |
|---------------|-------------|--------------------|--------------------|---------------------|---|
| 1 | 3 | UT-1 | 400/220 | 3 × 315 | Z1 = 0.14 pu; (X1/R1) = 20; Z0 = 0.14 pu; (X0/R0) = 20 |
| 2 | 4 | UT-2 | 400/220 | 2 × 315 | Z1 = 0.14 pu; (X1/R1) = 20; Z0 = 0.14 pu; (X0/R0) = 20 |
| 5 | 21 | UT-3 | 220/132 | 3 × 100 | Z1 = 0.12 pu; (X1/R1) = 20; Z0 = 0.12 pu; (X0/R0) = 20 |
| 8 | 20 | UT-4 | 220/132 | 260 | Z1 = 0.12 pu; (X1/R1) = 20; Z0 = 0.12 pu; (X0/R0) = 20 |
| 7 | 15 | UT-5 | 220/132 | 570 | Z1 = 0.12 pu; (X1/R1) = 20; Z0 = 0.12 pu; (X0/R0) = 20 |
| 6 | 14 | UT-6 | 220/132 | 160 | Z1 = 0.12 pu; (X1/R1) = 20; Z0 = 0.12 pu; (X0/R0) = 20 |
| 10 | 37 | UT-7 | 220/132 | 100 | Z1 = 0.12 pu; (X1/R1) = 20; Z0 = 0.12 pu; (X0/R0) = 20 |
| 9 | 26 | UT-8 | 220/132 kV | 260 | Z1 = 0.12 pu; (X1/R1) = 20; Z0 = 0.12 pu; (X0/R0) = 20 |
| 11 | 44 | UT-9 | 220/132 | 100 | Z1 = 0.12 pu; (X1/R1) = 20; Z0 = 0.12 pu; (X0/R0) = 20 |
| 12 | 46 | UT-10 | 220/132 | 2 × 100 | Z1 = 0.12 pu; (X1/R1) = 20; Z0 = 0.12 pu; (X0/R0) = 20 |
| 13 | 62 | UT-11 | 220/132 | 2 × 160 | Z1 = 0.12 pu; (X1/R1) = 20; Z0 = 0.12 pu; (X0/R0) = 20 |

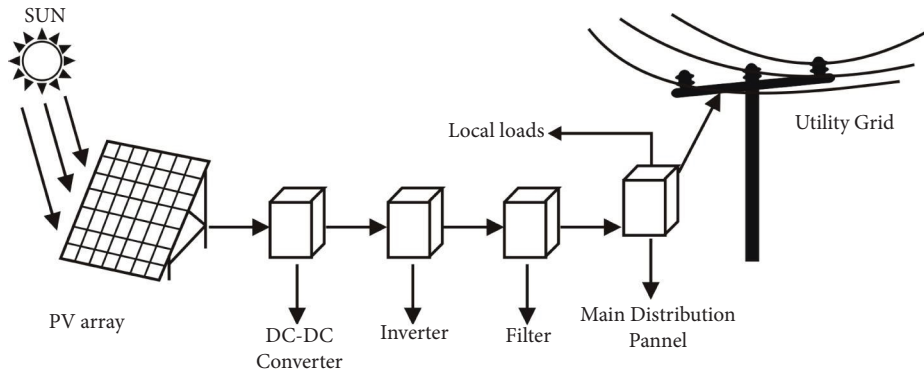


FIGURE 2: Basic structure of solar PV power plant.

TABLE 8: Average load recorded in last five years for the test system network.

| S. no. | Description | Years | | | | |
|--------|-----------------------------|--------|--------|---------|---------|----------|
| | | 2017 | 2018 | 2019 | 2020 | 2021 |
| 1 | Recorded average load (MW) | 947.44 | 984.29 | 1030.85 | 1080.13 | 1132.955 |
| 2 | Annual load growth rate (%) | — | 3.89% | 4.73% | 4.78% | 4.89% |

$$ul_k = P_m^{\max} + \frac{(P_m^{\max} - P_m^{\min})}{2 \times \text{NDOS}} \quad (11)$$

Objective space for the M number of objective function is divided into hyper boxes. The width w_k of hyper box in the k^{th} objective is described by the following relation:

$$w_k = \frac{(ul_k - ll_k)}{\text{NDOS}} \quad (12)$$

Grid coordinates of individuals in the objective are computed using the following relation.

$$G_k(x) = \frac{(f_k(k) - ll_k)}{w_k} \quad (13)$$

where $G_k(x)$ is grid coordinates of individual x in the k^{th} objective and $f_k(k)$ is actual objective value in the k^{th} objective.

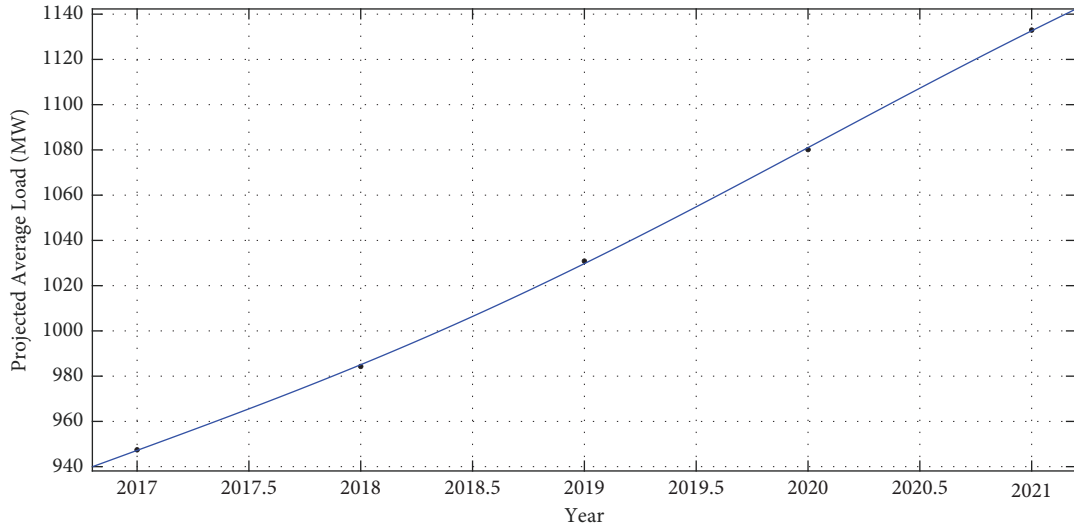


FIGURE 3: Load projection curve for ten year time horizon.

TABLE 9: Test network average load projection for ten years.

| Years | 2022 | 2023 | 2024 | 2025 | 2026 | 2027 | 2028 | 2029 | 2030 | 2031 |
|-----------------------------|--------|------|---------|---------|---------|---------|---------|---------|---------|---------|
| Projected average load (MW) | 1180.6 | 1219 | 1256.10 | 1298.70 | 1348.70 | 1401.10 | 1448.90 | 1489.10 | 1525.80 | 1566.50 |

To compute fitness, three grid dependent criteria such as grid ranking (GR), grid crowding distance, and grid coordinate point distance are used by the GOMOHSA to rank the individuals with better fitness. Convergence is computed utilizing the GR and grid coordinate point distance (GCPD). Grid crowding distance (GCD) is utilized for computing the diversity of entities. GR is expressed as summation of its grid coordinates in every objective:

$$GR_x = \sum_{k=1}^M G_k(x). \quad (14)$$

GCD takes care of density estimation and considers the distribution of neighbours of a solution. It is expressed by the following expression with condition that $G D(x, y) < M$

$$GCD(x) = \sum_{y \in N(x)} (M - G D(x, y)). \quad (15)$$

Euclidean distance among an individual and best corner solution of the respective hyper box is considered as GCPD which is computed using the following relation:

$$GCPD(x) = \sqrt{\sum_{k=1}^M F_k(x) - \left(\frac{lb_k + G_k(x) \times d_k}{d_k} \right)^2}. \quad (16)$$

The problem of optimal sizing and optimal location of RE generators in the practical network of the RVPN transmission system is solved by optimization of the following objective function using the GOMOHSA approach to minimize the active power loss (P_L), reactive power loss (Q_L), and total voltage deviations:

$$\min(APF, RPF, TVDF) = \text{Min}(P_L, Q_L, TVD). \quad (17)$$

The pareto multiobjective method is considered to solve the problem of DG units placement and sizing rather than a weighted sum-based multiobjective approach because total voltage deviations are primarily depended on the reactive power in the grid. However, TVD is also dependent on the loading of the lines relative to their surge impedance loading (SIL). Hence, parameters of the multiobjective function of the investigated problem are not absolutely independent of each other.

The proposed GOMOHSA used for solving the problem of optimal sizing and optimal location of RE generators in the practical transmission network of RVPN is summarized and illustrated in Figure 4.

4.3. Computation of Performance Function Indexes. The performance of the proposed method for loss minimization and voltage profile improvement in the practical transmission grid network by optimal sizing and deployment of RE generators is evaluated in terms of three performance indexes, namely, active power loss minimization index (APLMI), the reactive power loss minimization index (RPLMI), and the total voltage deviation improvement index (TVDMI). These three indexes are essentially required for overall health of the grid. Hence, all these three have equal importance for the assessment of the performance of the grid. These indexes are described in the following subsections.

4.3.1. Active Power Loss Minimization Indexes. The effectiveness of optimal sizing and deployment of RE generators using the grid-oriented multiobjective harmony search algorithm (GOMOHSA) on active power loss minimization is

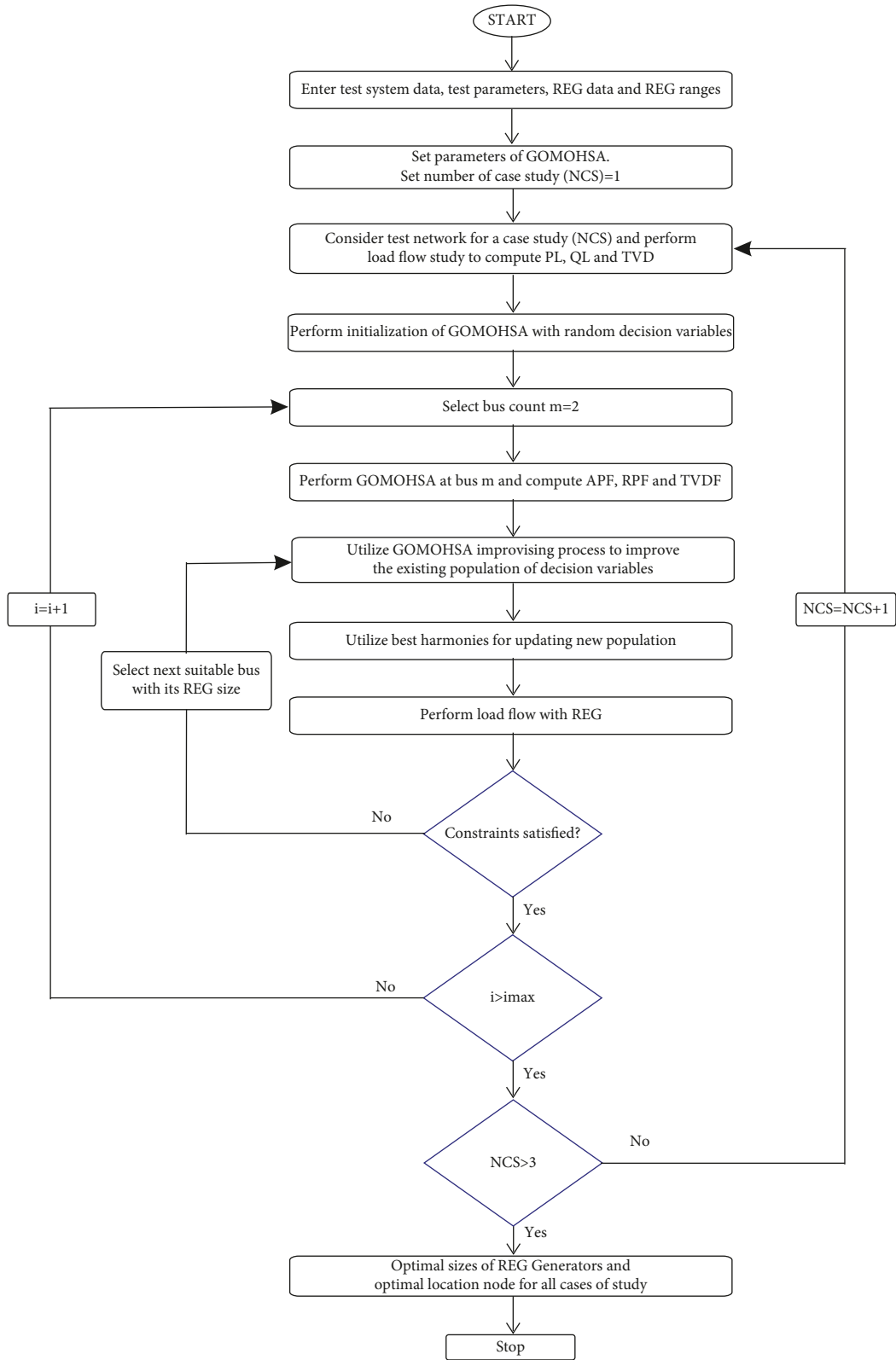


FIGURE 4: Illustration of proposed GOMOHSA.

evaluated in terms of APLMI. APLMI is expressed as a percentage ratio of total active power loss with RE generator placement (P_{LWRE}) to the total active power loss without RE generator placement (P_{LNRE}) as described by the following expression:

$$APMLI = \frac{P_{LWRE}}{P_{LNRE}} \times 100\%. \quad (18)$$

Lower the value of APLMI compared to 100%, the active power losses will be minimum. Hence, efficiency of the network to transmit power from generating stations to the load centers will be high.

4.3.2. Reactive Power Loss Minimization Index. The effectiveness of optimal sizing and deployment of RE generators using the grid-oriented multiobjective harmony search algorithm (GOMOHSA) on reactive power loss minimization is evaluated in terms of RPMLI. RPMLI is expressed as a percentage ratio of total reactive power loss with RE generator placement (Q_{LWRE}) to the total reactive power loss without RE generator placement (Q_{LNRE}) as described by the following expression:

$$RPMLI = \frac{Q_{LWRE}}{Q_{LNRE}} \times 100\%. \quad (19)$$

Lower the value of RPMLI compared to 100%, the reactive power losses will be minimum.

4.3.3. Total Voltage Deviation Improvement Index. The effectiveness of optimal sizing and deployment of RE generators using grid-oriented multiobjective harmony search algorithm (GOMOHSA) to minimize the voltage deviations at all buses of the network is evaluated in terms of TVDII. TVDII is expressed as a percentage ratio of total voltage deviation (summation of voltage deviations at all buses) with RE generator placement (ΔV_{LWRE}) to the total voltage deviation without RE generator placement (ΔV_{LNRE}) as described by the following expression:

$$TVDII = \frac{\Delta V_{LWRE}}{\Delta V_{LNRE}} \times 100\%. \quad (20)$$

Lower the value of TVDII compared to unity, the better will be the voltage profile. Lower value of TVDII helps to maintain voltage at each bus of the power system within the acceptable range.

5. Simulation Results and Discussion

Results without the deployment of RE generators and with the deployment of optimally sized RE generators for the scenarios of base year 2021 and projected year 2031 are discussed in this section. Results for all the investigated eight cases of study are discussed in this section.

5.1. Cases of Study. Performance of proposed method is evaluated considering two different scenario of the RVPN transmission network for base year 2021 and year 2031.

Further, for each of base year and projected year scenario study is performed with deployment of one, two and three RE generator units. All cases of networks considered for the study are detailed in the following:

- (i) Case-1: scenario of base year 2021 network without RE generator unit deployment.
- (ii) Case-1A: scenario of base year 2021 network with one RE generator unit deployment.
- (iii) Case-1B: scenario of base year 2021 network with two RE generator unit deployment.
- (iv) Case-1C: scenario of base year 2021 network with three RE generator unit deployment.
- (v) Case-2: scenario of projected year 2031 network without RE generator unit deployment.
- (vi) Case-2A: scenario of projected year 2031 network with one RE generator unit deployment.
- (vii) Case-2B: scenario of projected year 2031 network with two RE generator unit deployment.
- (viii) Case-2C: scenario of projected year 2031 network with three RE generator unit deployment.

5.2. Objective Function Values Using Simulation Study.

The proposed objective function, aimed to minimize total active power loss, total reactive power loss, and total voltage deviations of the network is optimized by application of GOMOHSA for all cases of study. Objective functions in Pareto optimal solutions for the condition of year 2021 without deployment of RE generators are illustrated in Figure 5. It is observed that the objective function is minimized with values of active power loss, reactive power loss, and maximum voltage deviation (MVD) equal to 7.27 MW, 17.31 MVAR, and 0.055 p.u., respectively. Optimized values of objective functions are included in Table 10.

Objective functions in Pareto optimal solutions for the condition of projected year 2031 without deployment of RE generators are illustrated in Figure 6. It is observed that the objective function is minimized with values of active power loss, reactive power loss, and maximum voltage deviation (MVD) equal to 13.94 MW, 33.18 MVAR, and 0.077 p.u., respectively. Optimized values of objective functions are included in Table 10.

Objective functions in Pareto optimal solutions for the condition of base year 2021 and projected year 2031 are also computed considering the deployment of one, two, and three RE generators. Optimized values of objective functions for all these cases of study are included in Table 10. Objective functions in pareto optimal solutions for the condition of base year 2021 considering one RE generator and for the condition of projected year 2031 considering three RE generators are illustrated in Figures 7 and 8, respectively. It is observed that the objective functions are minimized for each case with a set of values of active power loss, reactive power loss, and maximum voltage deviation (MVD).

The data included in Table 10 indicate that the deployment of optimally sized RE generators will improve the voltage profile of the network and it will reduce the active as

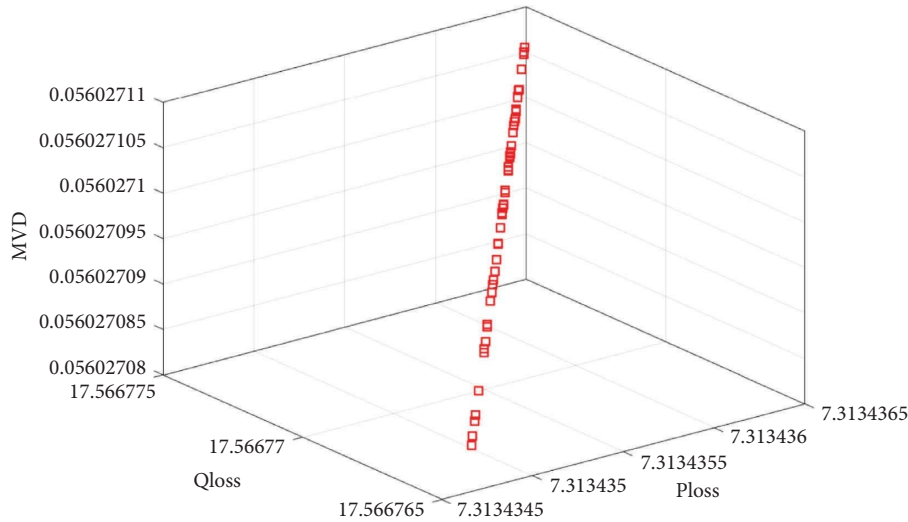


FIGURE 5: Objective functions in Pareto optimal solutions for the condition of year 2021 without deployment of RE generators.

TABLE 10: Objective function values.

| S. no. | Objective functions | Without REG units | | REG units with 2021 scenario | | | REG units with 2031 scenario | | |
|--------|----------------------------------|-------------------|-------|------------------------------|---------|-----------|------------------------------|---------|-----------|
| | | 2021 | 2031 | One REG | Two REG | Three REG | One REG | Two REG | Three REG |
| 1 | Total active power loss (MW) | 7.27 | 13.94 | 3.09 | 1.17 | 0.82 | 6.91 | 4.49 | 3.95 |
| 2 | Total reactive power loss (MVAR) | 17.31 | 33.18 | 7.35 | 2.79 | 1.94 | 16.44 | 10.68 | 9.41 |
| 3 | Total voltage deviation (p.u.) | 0.055 | 0.077 | 0.044 | 0.026 | 0.017 | 0.053 | 0.037 | 0.036 |

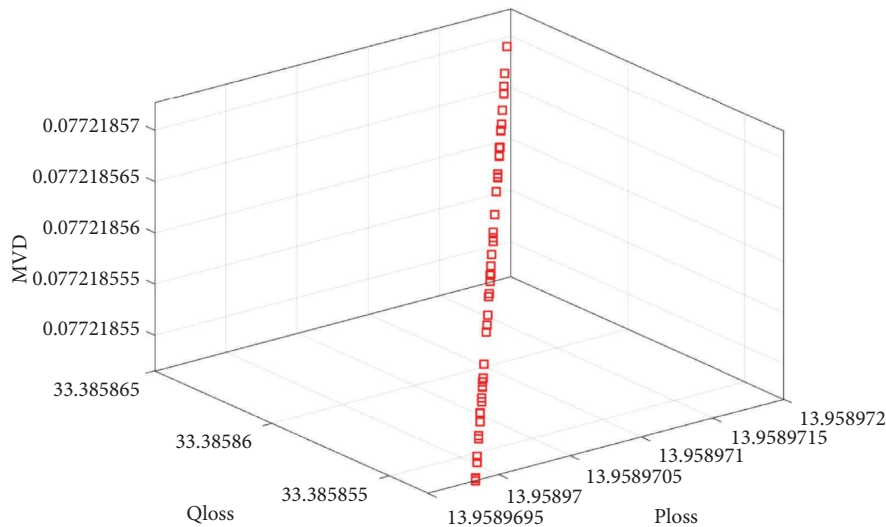


FIGURE 6: Objective functions in Pareto optimal solutions for the condition of year 2031 without deployment of RE generators.

well as reactive power losses in the network. Active power loss saving (APLS) in terms of MW and kWh are included in Table 11. Electricity saving (ES) in terms of kWh/year is computed using the following relation:

$$ES\left(\frac{\text{kWh}}{\text{year}}\right) = \text{APLS}(MW) \times 1000 \times 8760. \quad (21)$$

5.3. *Optimal Sizing and Placement of RE Generator Units.* Optimal sizing and network buses on which RE generators are proposed to be placed using the proposed method of GOMOHSA are included in Table 12. It is observed that the total capacity for placement of two RE generator units and three RE generator units is nearly the same. After, detailed analysis of data of suggested RE generator units, it is

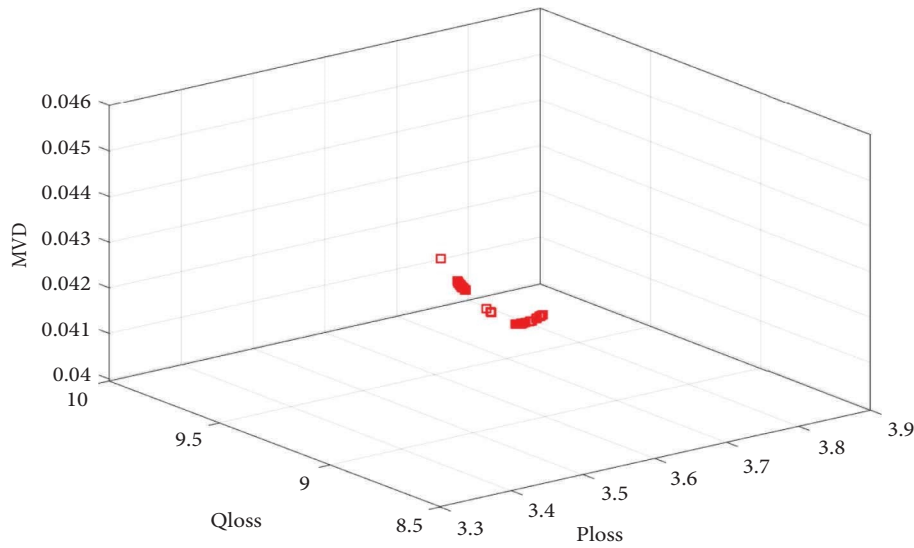


FIGURE 7: Objective functions in Pareto optimal solutions for the condition of year 2021 with deployment of one RE generator.

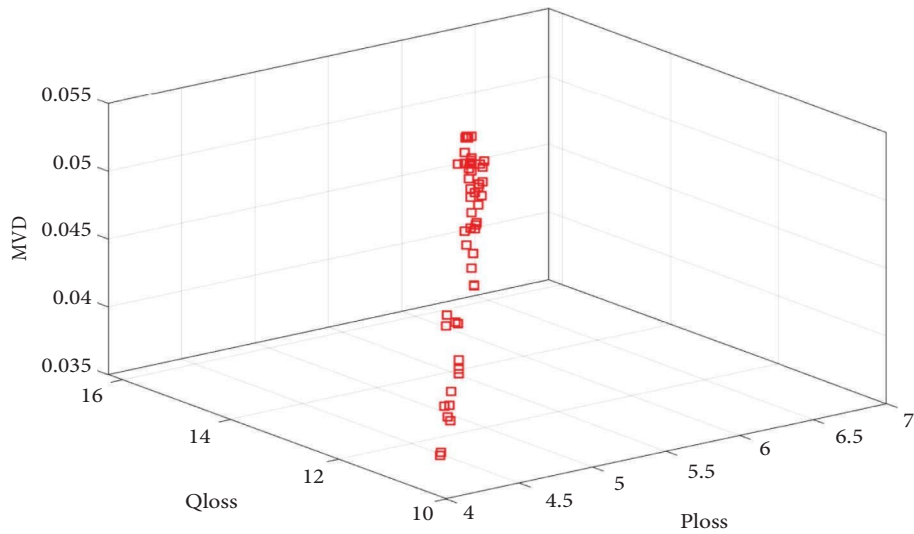


FIGURE 8: Objective functions in Pareto optimal solutions for the condition of year 2031 with deployment of three RE generators.

TABLE 11: Active power loss saving.

| S. no. | Particular | With respect to 2021 scenario | | | With respect to 2031 scenario | | |
|--------|---------------|-------------------------------|------------|------------|-------------------------------|------------|------------|
| | | One REG | Two REG | Three REG | One REG | Two REG | Three REG |
| 1 | APLS (MW) | 4.18 | 6.10 | 6.45 | 7.03 | 9.45 | 9.99 |
| 2 | ES (kWh/year) | 36,616,800 | 53,436,000 | 56,502,000 | 61,582,800 | 82,782,000 | 87,512,400 |

concluded that two RE generator units each of capacity 175 MW may be deployed on the network buses with numbers 51 and 63. Further, one unit of an RE generator with a capacity of 80 MW may be deployed on the network bus 25.

5.4. Analysis of Voltages on Network Buses. Voltages on nodes of network for the scenario of years 2021 and 2031 are analyzed without deployment of RE generator. The voltage

profile is also analyzed with the deployment of one, two, and three generators for each case of study. The voltage profile of network buses for the scenario of base year 2021 is illustrated in Figure 9. The voltage profile on network nodes for the scenario of year 2031 without deployment of RE generator units is also included in Figure 9.

In Figure 9, voltages on the network buses are reduced to be relatively large extent for the scenario of the projected year 2031 compared to the base year 2021. Further, improvement in network bus voltages is observed with the

TABLE 12: Optimal capacity of RE generators.

| S. no. | Bus no. | REG capacity with 2021 scenario (MW) | | | REG units with 2031 scenario (MW) | | | Optimal RE capacity (MW) |
|--------|-------------------|--------------------------------------|---------|-----------|-----------------------------------|---------|-----------|--------------------------|
| | | One REG | Two REG | Three REG | One REG | Two REG | Three REG | |
| 1 | 25 | — | — | — | — | — | 165.21 | 80 |
| 2 | 28 | — | — | 62.84 | — | — | — | — |
| 3 | 51 | — | 198.42 | 187.42 | 198.66 | 173.08 | 184.43 | 175 |
| 4 | 52 | 184.72 | — | — | — | — | 19.88 | — |
| 5 | 63 | — | — | 194.25 | — | — | — | 175 |
| 6 | 64 | — | 199.45 | — | — | — | — | — |
| 7 | 69 | — | — | — | — | 172.28 | — | — |
| 8 | Total RE capacity | 184.72 | 397.87 | 444.51 | 198.66 | 345.36 | 369.52 | 430 |

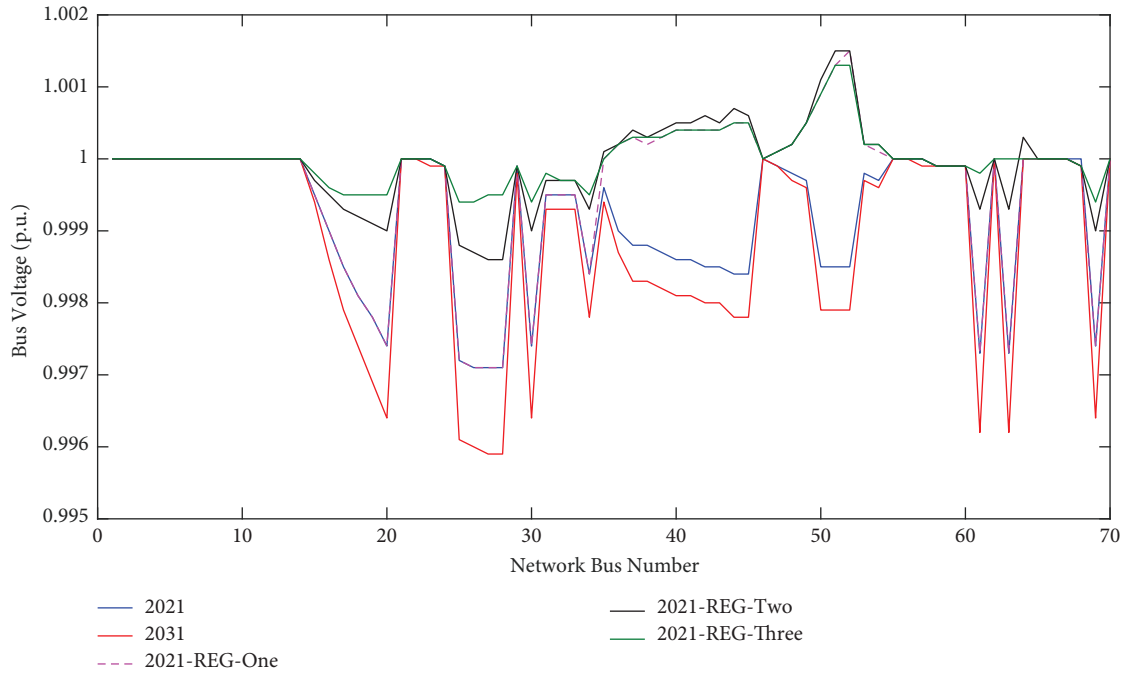


FIGURE 9: Voltage profile of network buses for the scenario of base year 2021.

deployment of RE generator units. Improvement in network bus voltages is highest for the deployment of three RE generator units and minimum with the deployment of one RE generator unit. Hence, it is concluded that optimal deployment of RE generator units of optimal size using the proposed method improves the voltage profile on the network buses.

The voltage profile of network buses for the scenario of the projected year 2031 with and without the deployment of RE generator units is illustrated in Figure 10. Figure 10 illustrates that an improvement in network bus voltages is observed with the deployment of RE generator units. Improvement in network bus voltages is highest for the deployment of three RE generator units and minimum with the deployment of one RE generator unit. Hence, it is concluded that optimal deployment of RE generator units of optimal sizes using the proposed method improves the voltage profile on the network buses for the projected year scenario.

5.5. Computation of Performance Index. Performance indexes, including APMLI, RPMLI, and TVDII are computed for all the cases of study and tabulated in Table 13. Base

parameters for both the cases of study are taken the parameters without deployment of RE generator units for the same case. It is observed that APMLI is maximum for both the cases of study with one RE generator deployment and minimum with the deployment of three RE generators. During the case-1 study, RPMLI is observed to be equal to 42.50, 16.09, and 11.28 with one, two, and three RE generator units, respectively. During the case-2 study, RPMLI is observed to be equal to 49.57, 32.21, and 28.33 with one, two and three RE generator units, respectively. Hence, maximum reduction in active power loss has been observed with deployment three RE generator units.

Table 13 depicts that RPMLI is maximum for both cases of study with one RE generator deployment and minimum with deployment of three RE generators. During the case-1 study, RPMLI is observed to be equal to 42.46, 16.12, and 11.21 with one, two, and three RE generator units, respectively. During the case-2 study, RPMLI is observed to be equal to 49.55, 32.19, and 28.36 with one, two, and three RE generator units, respectively. Hence, the maximum reduction in reactive power loss has been observed with the deployment of three RE generator units.

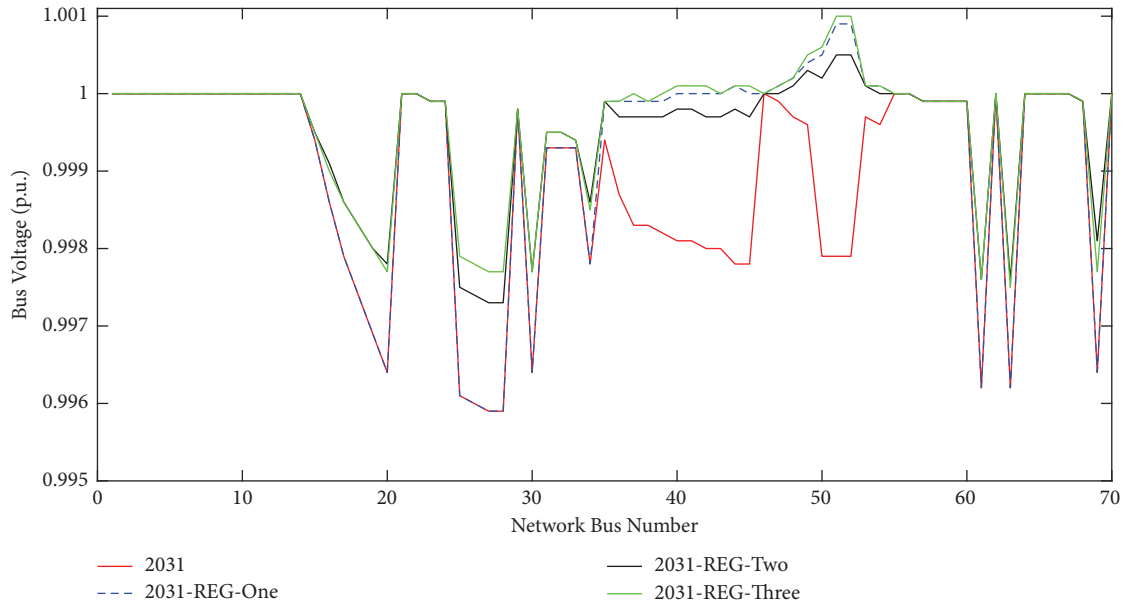


FIGURE 10: Voltage profile of network buses for the scenario of projected year 2031.

TABLE 13: Performance indexes.

| S. no. | Performance index | REG units with 2021 scenario | | | REG units with 2031 scenario | | |
|--------|-------------------|------------------------------|---------|-----------|------------------------------|---------|-----------|
| | | One REG | Two REG | Three REG | One REG | Two REG | Three REG |
| 1 | APMLI | 42.50 | 16.09 | 11.28 | 49.57 | 32.21 | 28.33 |
| 2 | RPMLI | 42.46 | 16.12 | 11.21 | 49.55 | 32.19 | 28.36 |
| 3 | TVDII | 80 | 47.27 | 30.90 | 68.83 | 48.05 | 46.75 |

Table 13 depicts that TVDII is maximum for both cases of study with one RE generator deployment and minimum with deployment of three RE generators. During the case-1 study, TVDII is observed to be equal to 80, 47.27, and 30.90 with one, two, and three RE generator units, respectively. During the case-2 study, TVDII is observed to be equal to 68.83, 48.05, and 46.75 with one, two, and three RE generator units, respectively. Hence, the maximum reduction in total voltage deviation has been observed with deployment three RE generator units. Further, total voltage deviations are minimized with the deployment of RE generator units. It is concluded that APMLI, RPMLI, and TVDII are minimized by the deployment of RE generator units and minimum values of these parameters are observed with the deployment of three RE generator units.

6. Analysis of Cost Benefits

The payback period is computed to recover the cost of the installation of RE generators for all cases of study. Electricity tariff (ET) for cost benefit computation is taken current tariff in India, which is equal to Indian Rupees (INR) 7.65/kWh [27]. Total installation cost for a RE generator (solar photovoltaic (PV) system) of capacity 10 kW is approximately equal to INR 82000 [28]. This cost includes the cost of wiring charges, operation, and maintenance costs.

Annual cost saving (ACS) due to electricity saving by deployment of RE generators is computed by the following relation:

$$ACS \left(\frac{\text{INR}}{\text{year}} \right) = ES \left(\frac{\text{kWh}}{\text{year}} \right) \times 7.65 \left(\frac{\text{INR}}{\text{kWh}} \right). \quad (22)$$

Total capital cost (TCC) for deployment of RE generator is expressed by the following relation:

$$TCC (\text{INR}) = \frac{\text{REGCapacity} (\text{MW}) \times 1000 \times 82000}{10}. \quad (23)$$

Payback period (PBP) is defined as ratio of total capital cost (TCC) incurred on deployment of RE generators to annual cost saving as described in the following [29]:

$$\text{PBP} (\text{year}) = \frac{\text{TCC}}{\text{ACS}}. \quad (24)$$

Annual cost saving, total capital cost and payback period for all cases of study for deployment of RE generators are included in Table 14.

Table 14 depicts that the payback period for the deployment of two RE generators and three RE generators is approximately the same for the base year 2021 and the projected year 2031. However, performance parameters are improved by the deployment of three RE generators. Further, the payback period for RE generator deployment

TABLE 14: Active power loss saving and payback period.

| S. no. | Particulars | With respect to year 2021 scenario | | | With respect to year 2031 scenario | | |
|--------|----------------|------------------------------------|---------------|---------------|------------------------------------|---------------|---------------|
| | | One REG | Two REG | Three REG | One REG | Two REG | Three REG |
| 1 | ACS (INR/year) | 280,118,520 | 408,785,400 | 432,240,300 | 471,108,420 | 633,282,300 | 669,469,860 |
| 2 | TCC (INR) | 1,514,704,000 | 3,262,534,000 | 3,644,982,000 | 1,629,012,000 | 2,831,952,000 | 3,030,064,000 |
| 2 | PBP (year) | 5.407 | 7.981 | 8.433 | 3.458 | 4.472 | 4.526 |

during the base year is approximately 8 years and 4.5 years for the projected year 2031. Hence, it is concluded that three RE generators may be deployed in the base year to get the maximum benefit in terms of cost savings.

7. Performance Comparison

Performance of the proposed GOMOHSA is established for the deployment of RE generators in a practical transmission system of RVPN by comparing it with the performance of the genetic algorithm (GA) reported in [30] for the deployment of RE generators in the RVPN transmission network used for the study. The performance comparative study for deployment of three RE generators for the condition of projected year 2031 using the proposed GOMOHSA and GA reported in [30] is included in Table 15.

Table 15 depicts that the RE generator capacity for deployment of three generators using GOMOHSA and GA are 369.52 MW and 475.28 MW, respectively. Higher capacity of RE generator is estimated using GA compared to the GOMOHSA. Active power loss savings are 9.99 MW and 6.92 MW by deployment of three RE generators using GOMOHSA and GA, respectively. Hence, APLS is high by application of GOMOHSA compared to the GA. The payback period to recover the capital cost for deployment of RE generators using GOMOHSA and GA is 4.526 year and 8.404 year, respectively. Hence, capital cost will be recovered earlier with the use of GOMOHSA.

7.1. Sensitivity Analysis. Parameter sensitivity analysis is performed for both the GOMOHSA and GA considering a placement of three DG units each rated at capacity of 50 MW and 20 MVAR for condition of projected year 2031. The rate of change of active power loss (APL) with respect to change in active power (P) injection by DG and the rate of change of total voltage deviation (TVD) with respect to a change in reactive power (Q) injection are considered to analyze the parameter sensitivity of the methods. The rate of change of active power loss (APL) (ΔAPL) with respect to active power (P) injection by DG (ΔP) is defined by the following relation:

$$\frac{\Delta APL}{\Delta P} = \frac{\text{Total Change in Active Power Loss}}{\text{Total Change in Active Power Injection}} \quad (25)$$

Rate of change of total voltage deviation (TVD) (ΔTVD) with respect to reactive power (Q) injection by DG (ΔQ) is defined by the following relation:

TABLE 15: Performance comparison of GOMOHSA and GA.

| S. no. | Parameters | GOMOHSA | GA [30] |
|--------|-------------------|---------|---------|
| 1 | APMLI | 28.33 | 37.48 |
| 2 | RPMLI | 28.36 | 38.10 |
| 3 | TVDII | 46.75 | 55.28 |
| 4 | REG capacity (MW) | 369.52 | 475.28 |
| 5 | APLS (MW) | 9.99 | 6.92 |
| 6 | PBP (Year) | 4.526 | 8.404 |

TABLE 16: Parameter sensitivity of GOMOHSA and GA.

| S. no. | Sensitivity criteria | GOMOHSA | GA [30] |
|--------|-----------------------|---------|---------|
| 1 | $\Delta APL/\Delta P$ | 0.01072 | 0.01980 |
| 2 | $\Delta TVD/\Delta Q$ | 0.01950 | 0.02804 |

$$\frac{\Delta TVD}{\Delta Q} = \frac{\text{Change of Total Voltage Deviation}}{\text{Total Change in Reactive Power Injection}} \quad (26)$$

Sensitivity analysis is performed by changing the capacity of each DG unit to 60 MW and 25MVAR. Sensitivity analysis is illustrated in Table 16.

The active power loss rate change is 1.847 times higher for the DG placement using GA compared to GOMOHSA. Similarly, the total voltage deviation rate change is 1.438 times higher for the DG placement using GA compared to GOMOHSA. Therefore, it is concluded that the proposed GOMOHSA is less sensitive to the parameter variations compared to the GA reported in [30].

8. Conclusions

This paper presented a grid-oriented multiobjective harmony search algorithm for optimal placement and sizing of the RE generators in a part of the RVPN transmission network to minimize the active power loss, reactive power loss, and improvement of voltage profile. This is concluded that the optimal sizes of one, two, and three RE generators for the base year 2021 is found to be 184.72 MW, 397.87 MW, and 444.51 MW, respectively. Similarly, the respective values for the projected year 2031 are 198.66 MW, 345.36 MW, and 369.52 MW. Voltage profile has improved for the base year and projected year after placement of RE generators. Magnitudes of performance indexes, including APMLI, RPMLI, and TVDII has magnitudes in descending order with one REG, two REG, and three REG units for the scenario of both base year and projected year. This has

indicated that health of grid network has improved by REG placement and maximum effect is observed with three REG units. The payback period for the placement of one REG, two REG, and three REG for the base year is found to be 5.407 year, 7.981 year, and 8.433 year, respectively. Similar values for the projected year are 3.458 year, 4.472 year, and 4.526 year. Recommended capacity of RE generators are 80 MW, 175 MW, and 175 MW on the nodes 25, 51, and 63, respectively of the test system. The performance of the proposed GOMOHSAs is better compared to the conventional genetic algorithm (GA) in terms of performance indexes, RE generator capacity, payback period, and sensitivity of parameters.

Abbreviations

| | |
|-----------|---|
| ABC: | Artificial bee colony |
| AC: | Alternating current |
| ACS: | Annual cost saving |
| ACSR: | Aluminium conductor steel reinforced |
| ALGR: | Average annual load growth rate |
| APF: | Active power loss minimization function |
| APL: | Active power loss |
| APLS: | Active power loss saving |
| APMLI: | Active power loss minimization index |
| BESS: | Battery Energy Storage System |
| D/C: | Double circuit |
| DDG: | Dispatchable distributed generations |
| ES: | Electricity saving |
| ET: | Electricity tariff |
| FL: | Fuzzy logic |
| FY: | Financial year |
| GA: | Genetic algorithm |
| GCD: | Grid crowding distance |
| GCPD: | Grid coordinate point distance |
| GR: | Grid ranking |
| DC: | Direct current |
| DG: | Distributed generation |
| GOMOHSAs: | Grid-oriented multiobjective harmony search algorithm |
| GSS: | Grid substation |
| HSA: | Harmony search algorithm |
| IEEE: | Institute of Electrical and Electronics Engineering |
| INR: | Indian Rupees |
| MATLAB: | Matrix laboratory |
| MPSI: | Maximum power stability index |
| MVD: | Maximum voltage deviation |
| NDOS: | Number of divisions of objective space |
| OLI: | Optimal locator index |
| PABC: | Particle artificial bee colony algorithm |
| PAL: | Projected average load |
| PBP: | Payback period |
| PGCIL: | Power-grid corporation of India limited |
| PV: | Photovoltaic |
| PSI: | Power stability index |
| PSO: | Particle swarm optimization |
| RMSE: | Root mean square error |
| RE: | Renewable energy |

| | |
|--------|---|
| REG: | Renewable energy generator |
| RPF: | Reactive power loss minimization function |
| RPMLI: | Reactive power loss minimization index |
| RVPN: | Rajasthan Rajya Vidyut Prasaran Nigam Limited |
| S/C: | Single circuit |
| SIL: | Surge impedance loading |
| SPP: | Solar photovoltaic power plant |
| SSE: | Summation of squared estimate of errors |
| TCC: | Total capital cost |
| TVD: | Total voltage deviations |
| TVDF: | Total voltage deviation minimization function |
| TVDII: | Total voltage deviation improvement index. |

Data Availability

The data are available from the corresponding author upon reasonable request.

Conflicts of Interest

The authors declare that they have no conflicts of interest.

Acknowledgments

The researchers would like to acknowledge Deanship of Scientific Research, Taif University for funding this work.

References

- [1] S. Ravindran and T. A. A. Victoire, "A bio-geography-based algorithm for optimal siting and sizing of distributed generators with an effective power factor model," *Computers and Electrical Engineering*, vol. 72, pp. 482–501, 2018.
- [2] S. H. Lee and J. W. Park, "Optimal placement and sizing of multiple DGs in a practical distribution system by considering power loss," *IEEE Transactions on Industry Applications*, vol. 49, no. 5, pp. 2262–2270, 2013.
- [3] H. Alsharif, M. Jalili, and K. N. Hasan, "Power system frequency stability using optimal sizing and placement of Battery Energy Storage System under uncertainty," *Journal of Energy Storage*, vol. 50, Article ID 104610, 2022.
- [4] R. Ishak, A. Mohamed, A. N. Abdalla, and M. Z. Che Wanik, "Optimal placement and sizing of distributed generators based on a novel MPSI index," *International Journal of Electrical Power and Energy Systems*, vol. 60, pp. 389–398, 2014.
- [5] K. Prakash, F. R. Islam, K. A. Mamun, and S. Ali, "Optimal Generators Placement Techniques in Distribution Networks: A Review," in *Proceedings of the 2017 Australasian Universities Power Engineering Conference (AUPEC)*, pp. 1–6, Melbourne, VIC, Australia, November 2017.
- [6] R. Shivarudraswamy and D. N. S. J. Gaonkar, "GA based optimal location and size of the distributed generators in distribution system for different load conditions," in *Proceedings of the 2016 IEEE 1st International Conference on Power Electronics, Intelligent Control and Energy Systems (ICPEICES)*, pp. 1–4, Delhi, India, July 2016.
- [7] R. Vempalle and P. K. Dhal, "Maximization of economy in distribution networks with most favorable placement of type-1 and type-2 distributed generators along with reorganization

- using PSO-WOA hybrid optimization algorithm,” *ARNP Journal of Engineering and Applied Sciences*, vol. 16, no. 22, 2021.
- [8] P. P. Biswas, R. Mallipeddi, P. Suganthan, and G. A. Amaratunga, “A multiobjective approach for optimal placement and sizing of distributed generators and capacitors in distribution network,” *Applied Soft Computing*, vol. 60, pp. 268–280, 2017.
- [9] P. D. Huy, V. K. Ramachandaramurthy, J. Y. Yong, K. M. Tan, and J. B. Ekanayake, “Optimal placement, sizing and power factor of distributed generation: a comprehensive study spanning from the planning stage to the operation stage,” *Energy*, vol. 195, Article ID 117011, 2020.
- [10] K. Muthukumar and S. Jayalalitha, “Optimal placement and sizing of distributed generators and shunt capacitors for power loss minimization in radial distribution networks using hybrid heuristic search optimization technique,” *International Journal of Electrical Power and Energy Systems*, vol. 78, pp. 299–319, 2016.
- [11] M. Othman, W. El-Khattam, Y. Hegazy, and A. Y. Abdelaziz, “Optimal placement and sizing of voltage controlled distributed generators in unbalanced distribution networks using supervised firefly algorithm,” *International Journal of Electrical Power and Energy Systems*, vol. 82, pp. 105–113, 2016.
- [12] T. Vinod Kumar and S. Kumar Injeti, “Probabilistic optimal planning of dispatchable distributed generator units in distribution systems using a multi-objective velocity-based butterfly optimization algorithm,” *Renewable Energy Focus*, vol. 43, pp. 191–209, 2022.
- [13] M. Yehia, D. Allam, and A. F. Zobaa, “A novel hybrid fuzzy-metaheuristic strategy for estimation of optimal size and location of the distributed generators,” *Energy Reports*, vol. 8, pp. 12408–12425, 2022.
- [14] G. Chen, B. Chen, P. Dai, and H. Zhou, “A sustainability-oriented multiobjective optimization model for siting and sizing distributed generation plants in distribution systems,” *Mathematical Problems in Engineering*, vol. 2013, Article ID 291930, 11 pages, 2013.
- [15] T. R. Ayodele, A. S. O. Ogunjuyigbe, and O. O. Akinola, “Optimal location, sizing, and appropriate technology selection of distributed generators for minimizing power loss using genetic algorithm,” *Journal of Renewable Energy*, vol. 2015, Article ID 832917, 9 pages, 2015.
- [16] L. C. Kien, T. T. Bich Nga, T. M. Phan, and T. T. Nguyen, “Coot optimization algorithm for optimal placement of photovoltaic generators in distribution systems considering variation of load and solar radiation,” *Mathematical Problems in Engineering*, vol. 2022, Article ID 2206570, 17 pages, 2022.
- [17] RVPN, “Rajasthan Rajya Vidyut Prasaran Nigam Limited,” 2022, <https://energy.rajasthan.gov.in>.
- [18] S. R. Ola, A. Saraswat, S. K. Goyal, S. Jhaharia, B. Rathore, and O. P. Mahela, “Wigner distribution function and alienation coefficient-based transmission line protection scheme,” *IET Generation, Transmission and Distribution*, vol. 14, no. 10, pp. 1842–1853, 2020.
- [19] E. Kaushik, V. Prakash, O. P. Mahela et al., “Optimal placement of renewable energy generators using grid-oriented genetic algorithm for loss reduction and flexibility improvement,” *Energies*, vol. 15, no. 5, p. 1863, 2022.
- [20] Central Electricity Authority, “Transmission planning criteria,” 2021, <https://cea.nic.in/transmission-planning-criteria/?lang=en>.
- [21] O. P. Mahela and A. G. Shaik, “Detection of power quality events associated with grid integration of 100kW solar PV plant,” in *Proceedings of the 2015 International Conference on Energy Economics and Environment (ICEEE)*, pp. 1–6, Greater Noida, India, March 2015.
- [22] O. P. Mahela and A. G. Shaik, “Comprehensive overview of grid interfaced solar photovoltaic systems,” *Renewable and Sustainable Energy Reviews*, vol. 68, pp. 316–332, 2017.
- [23] O. P. Mahela and A. G. Shaik, “Power quality recognition in distribution system with solar energy penetration using S-transform and Fuzzy C-means clustering,” *Renewable Energy*, vol. 106, pp. 37–51, 2017.
- [24] O. Axelsson, “A generalized conjugate gradient, least square method,” *Numerische Mathematik*, vol. 51, no. 2, pp. 209–227, 1987.
- [25] G. Chen, Z. I. Ren, H. Z. Sun, and others, “Curve fitting in least-square method and its realization with Matlab,” *Ordinance industry automation*, vol. 3, p. 063, 2005.
- [26] K. S. Lee and Z. W. Geem, “A new meta-heuristic algorithm for continuous engineering optimization: harmony search theory and practice,” *Computer Methods in Applied Mechanics and Engineering*, vol. 194, no. 36–38, pp. 3902–3933, 2005.
- [27] Rajasthan Electricity Regulatory Commission, “Tariff For Supply of Electricity,” 2020, <https://energy.rajasthan.gov.in/content/raj/energy-department/en/departments/jvvn/Tarifforders.html>.
- [28] Loom Solar, “Solar Panel Installation Cost in India,” 2021, <https://www.loom solar.com/blogs/collections/solar-panel-installation-cost-in-india>.
- [29] T. F. Agajie, B. Khan, H. H. Alhelou, and O. P. Mahela, “Optimal expansion planning of distribution system using grid-based multi-objective harmony search algorithm,” *Computers and Electrical Engineering*, vol. 87, Article ID 106823, 2020.
- [30] M. Vatani, D. Solati Alkaran, M. J. Sanjari, and G. B. Gharehpetian, “Multiple distributed generation units allocation in distribution network for loss reduction based on a combination of analytical and genetic algorithm methods,” *IET Generation, Transmission and Distribution*, vol. 10, no. 1, pp. 66–72, 2016.